Communications in Information and Systems
Volume 13, Number 3, 291–325, 2013

The alternating evolution methods for first order nonlinear partial differential equations

Hailiang Liu

Dedicated to Marshall Slemrod with friendship and appreciation

In this paper, we present a brief survey of the recent developments in alternating evolution (AE) methods for numerical computation of first order partial differential equations, with hyperbolic conservation laws and Hamilton-Jacobi equations as two canonical examples. The main difficulty of such computation arises from the nonlinearity of the model, making it necessary to incorporate an appropriate amount of numerical viscosity to capture the entropy/viscosity solution as physically relevant solutions. The alternating evolution method is based on the AE system of the original PDEs, the discretization technique ranges from finite difference, finite volume and the discontinuous Galerkin methods. In all these cases, the AE solver can produce accurate solutions with equal computational time than the traditional solvers. In particular, the AE formulation allows the same discontinuous Galerkin discretization for both conservative and non-conservative PDEs under consideration. In order to make the presentation more concise and to highlight the main ideas of the algorithm, we use simplified models to describe the details of the AE method. Sample simulation results on a few models are also given.

1991 Mathematics Subject Classification: 35K15, 65M15, 65M60, 76R50.
Keywords and phrases: Conservation laws, Hamilton-Jacobi equations, alternating evolution methods, Lax-Friedrichs.

1. Introduction

In mathematics, a first-order partial differential equation (PDE) is an equation that involves only first order derivatives of the unknown function of multiple variables. The equation may take the form

$$F(\xi, \phi, \nabla_\xi \phi) = 0.$$

Such equations arise in the construction of characteristic surfaces for hyperbolic partial differential equations, in the calculus of variations, in some geometrical problems, and in simple models for gas dynamics whose solution involves the method of characteristics. For the resolutions of the underlying application problems, it has been shown to be important to analyze and solve the governing PDEs. For time dependent problems we distinguish the temporal variable $t > 0$ from the spatial variable $x \in \mathbb{R}^d$, and a first order PDE may be symbolically written as

$$\partial_t \phi + A(\phi) = 0, \quad x \in \mathbb{R}^d, \quad t > 0,$$

where A is a nonlinear differential operator. Two classes of PDEs are of particular interest: hyperbolic conservation laws $A = \nabla_x \cdot f(\phi)$ and Hamilton-Jacobi equations $A = H(x, \nabla_x \phi)$, which will be used to illustrate the main ideas of the alternation evolution (AE) methods in this article.

1.1. Hyperbolic conservation laws $A = \nabla_x \cdot f(\phi)$

A multi-dimensional hyperbolic conservation law has the form:

$$\partial_t \phi + \nabla_x \cdot f(\phi) = 0, \quad x \in \mathbb{R}^d, \quad t > 0, \tag{1}$$

where $\phi \in \mathbb{R}^m$ denotes a vector of conserved quantities, and $f : \mathbb{R}^m \to \mathbb{R}^d$ is a nonlinear convection flux. The compressible Euler equation in gas dynamics is a canonical example. These equations are of great practical importance since they model a variety of physical phenomena that appear in fluid mechanics, astrophysics, groundwater flow, traffic flow, semiconductor device simulation, and magneto-hydrodynamics, among many others.

The notorious difficulty encountered for the satisfactory approximation of the exact solutions of these systems lies in the presence of discontinuities in the solution, leading to non-uniqueness of the weak solution. We are interested in computing the physically relevant solution – so called the entropy solution. The entropy solution ϕ is defined so that ϕ satisfies the entropy inequalities

$$\int_0^\infty \int_{\mathbb{R}^d} (\eta(\phi)\partial_t v + q(\phi) \cdot \nabla_x v) dx dt \geq 0 \tag{2}$$

for each $v \in C_0^\infty(\mathbb{R}^d \times (0, \infty)$ and $v \geq 0$ and each entropy/entropy flux pair (η, q): η is convex and

$$D\eta(z) \cdot Df_j(z) = Dq_j(z), \quad j = 1 \cdots d.$$

1.2. Hamilton-Jacobi equations $A = H(x, \nabla_x \phi)$

Another important class is the Hamilton-Jacobi equation:

$$\partial_t \phi + H(x, \nabla_x \phi) = 0, \quad \phi(x, 0) = \phi_0(x), \quad x \in \mathbb{R}^d, \quad t > 0. \tag{3}$$

Here the unknown ϕ is scalar, and $H : \mathbb{R}^d \to \mathbb{R}^1$ is a nonlinear Hamiltonian. The Hamilton-Jacobi equation arises in many applications ranging from geometrical optics to differential games. These nonlinear equations typically develop discontinuous derivatives even with smooth initial conditions, such weak solutions are not unique.

It would be natural to try to extend the entropy solution concept based on integration by parts in (2) to Hamilton-Jacobi equations, unfortunately, attempts as such had gone fruitless until the first breakthrough in 1983 when Crandall and Lions introduced the notion of viscosity solutions and established their theory for Hamilton-Jacobi equations, see [9, 5, 59]. In the concept of viscosity solutions, the derivative of the solution is compared to a fixed test function at certain points via the comparison principle. A bounded uniformly continuous function ϕ is called a viscosity subsolution (supersolution) of (3) if, for every point (x_0, t_0) and a function $v \in C^\infty$ satisfying $\phi \leq (\geq) v$ and $\phi(x_0, t_0) = v(x_0, t_0)$, there holds

$$\partial_t v + H(x, \nabla_x v) \leq 0 \quad \text{at } (x_0, t_0).$$

Moreover, ϕ is called a viscosity solution if ϕ is simultaneously a viscosity subsolution and a viscosity supersolution.

We are interested in computation of the viscosity solution, which is the unique physically relevant solution in some important applications. The difficulty encountered for the satisfactory approximation of the exact solutions of these equations lies in the presence of discontinuities in the solution derivatives.

1.3. Numerical methods

Numerical discretization methods for first order PDEs are diverse, the popular ones are finite difference methods, finite volume methods and the discontinuous Galerkin methods.

Among the considerable amount of literature available on numerical methods for hyperbolic conservation laws and Hamilton-Jacobi equations,

the discretization solution techniques fall under two main categories according to their way of *sampling* [52]: upwind and central schemes. The forerunners for these two classes of high resolution schemes for conservation laws are the first order Godunov [17] and Lax-Friedrichs (LxF) schemes [16, 33], respectively. The need for devising more accurate and efficient numerical methods for conservation laws and related models has prompted and sustained the abundant research in this area, see, for example, [34, 61, 60, 7].

The success of high resolution schemes has been due to two factors: the local enforcement of the underlying PDE and the non-oscillatory piecewise polynomial reconstruction from evolved local moments (cell averages or gird values).

For conservation laws, various higher-order extensions of the Godunov type finite volume scheme have been rapidly developed since 1970's, employing higher-order reconstruction of piece-wise polynomials from the cell averages, including MUSCL, TVD, PPM, ENO and WENO schemes [62, 63, 19, 8, 20, 57, 58, 44]. In this development, the local refinement of one dimensional conservation laws may be expressed as

$$\partial_t \phi + \partial_x \hat{f}(\phi_-, \phi_+) = 0, \tag{4}$$

where $\hat{f}$ is an entropy satisfying numerical flux.

For Hamilton-Jacobi equations, the ENO/WENO type schemes ([24, 35, 54, 55, 56, 53, 65]) are based mainly on some local refinement of H-J equations by

$$\partial_t \phi + \hat{H}(x, \phi_x^+, \phi_x^-) = 0, \tag{5}$$

where $\hat{H}$ is the numerical Hamiltonian which needs to be carefully chosen to ensure that the viscosity solution is captured when ϕ_x becomes discontinuous.

In contrast, central type schemes such as the LxF scheme are more diffusive, yet easy to formulate and implement since no Riemann solvers are required. Examples of such schemes for conservation laws are the second-order Nessyahu-Tadmor scheme [52] and other higher-order schemes [45, 1, 36, 25, 30, 23]. For H-J equations, the central type schemes ([2, 3, 4, 29, 32, 38, 39]) choose to evolve the constructed polynomials in smooth regions so that the Taylor expansion may be used in the scheme derivation.

The two categories of the existing high resolution schemes are somehow interlaced during their independent developments; the upwind scheme becomes Riemann solver-free when a local numerical flux can be identified to

replace the exact Riemann solver, see Shu and Osher [57, 58], and the central scheme becomes less diffusive when variable control volumes are used in deriving the scheme, see Kurganov and Tadmor [31]. The upwind feature can be further enforced [21, 29] in central-upwind schemes, see [28] for a recent derivation of such a scheme. The relaxation scheme of Jin and Xin [26] provides yet another approach for solving nonlinear conservation laws, see also [27, 51].

The discontinuous Galerkin (DG) method has the advantage of flexibility for arbitrarily unstructured meshes, and with the ability to easily achieve arbitrary order of accuracy. The DG method has been quite successful for conservation laws [10, 11, 12, 13, 14] due to the conservative nature of the formulation (4). However, new difficulties occur when the existing ideas with finite difference methods are applied toward the discontinuous Galerkin discretization for the Hamilton-Jacobi equation (5). One main difficulty comes from the non-conservative form of (5), which precludes the use of integration by parts to establish the cell to cell communication via numerical fluxes as usually done with the DG methods for conservation laws. In spite of this difficulty, some progress has been made in past years, see [22, 6, 37, 64]. With the alternating evolution framework reviewed in this article, one can apply the same DG discretization to both conservation laws and Hamilton-Jacobi equations.

1.4. The alternating evolution (AE) system

The difference between the AE schemes discussed in this article and the existing schemes mentioned above lies in the local enforcement of underlying PDEs. Instead of using either (4) or (5), we refine the original PDE by an alternating evolution (AE) system

$$\partial_t u + \tilde{A}(u, v) = \frac{1}{\epsilon}(v - u),$$
$$\partial_t v + \tilde{A}(v, u) = \frac{1}{\epsilon}(u - v),$$

which involves two representatives: $\{u, v\}$. Here $\tilde{A}$ is a refinement of A so that terms involving spatial derivatives are replaced by v's derivatives, the additional relaxation term $(v - u)/\epsilon$, serves to communicate the two representatives u and v, with $\epsilon > 0$ being a scale parameter of user's choice. This amount of leverage in the choice of ϵ adds another attractive feature of the AE scheme. Indeed different choices of the scale parameter in such a

procedure yield different AE schemes [41]. We have $\tilde{A}(u,v) = \nabla_x \cdot f(v)$ for conservation laws, and $\tilde{A}(u,v) = H(x, \nabla_x v)$ for Hamilton-Jacobi equations.

The AE system for scalar hyperbolic conservation laws was originally proposed in [40], where the system was shown to be capable of capturing the exact solution when initially both representatives are chosen as the given initial data. Such a feature allows for a sampling of two representatives over alternating grids/cells. Using this alternating system as a 'building base', we apply standard approximation techniques to the AE system: high order accuracy is achieved by a combination of high-order non-oscillatory polynomial approximation in space and an ODE solver in time with matching accuracy. For conservation laws we sample using cell averages [40, 41] and for Hamilton-Jacobi equation we sample using grid values [42], which correspond to finite volume and finite difference schemes, respectively. For the discontinuous Galerkin discretization, same sampling of local moments is applied to both types of equations [43].

The procedure using the AE formulation opens a new way to derive robust highly accurate schemes for nonlinear PDEs, conservative or non-conservative. The AE schemes are very easy to implement and efficient. Actually such simplicity in implementation is even more pronounced in the multi-dimensional case.

More closely related to the AE scheme is the overlapping cell schemes introduced by Liu [46], who generalizes the NT scheme [52] by evolving two pieces of information over redundant overlapping cells, therefore allows for easy formulation of semi-discrete schemes. The technique has been extended to the development of some central discontinuous Galerkin methods for conservation laws and diffusion equations [47, 48, 49, 50], as well as for Hamilton-Jacobi equations [37]. One main difference between the overlapping central schemes and the AE schemes is that central overlapping schemes use two polynomial representatives solved on two sets of overlapping meshes, and the AE schemes only have one polynomial representative associated with each grid point, even in multi-dimensional case. The advantage of the AE scheme is clearer in the multi-dimensional case.

It should be noted that even though our AE schemes are derived based on sampling the alternating evolution system, we do not solve the system directly. The AE system simply provides a systematic way for developing numerical schemes of both semi-discrete and fully discrete form for the underlying PDEs, instead of as an approximation system at the continuous level.

The remainder of the article is organized as follows. In section 2, we illustrate how to derive the alternating evolution system from the Lax-Friedrichs

scheme for one-dimensional conservation laws. We formulate the high resolution finite volume AE schemes for hyperbolic conservation laws ([41]) in section 3, and high resolution finite difference AE schemes for Hamilton-Jacobi equations ([42]) in section 4. In section 5, we present high order AEDG schemes for both Hamilton-Jacobi equations ([43]) and hyperbolic conservation laws. Sample simulation results on a few models are given in section 6. The last section 7 ends this paper with some concluding remarks.

2. From the Lax-Friedrichs scheme to the AE system

The AE system was motivated by the Lax-Friedrichs scheme, as described in [40]. We start with finite difference schemes for one dimensional scalar hyperbolic conservation laws

$$\partial_t U + \partial_x f(U) = 0. \tag{6}$$

Let the xt-plane be covered by a rectangular gird with mesh size Δx in $x-$direction and Δt in the $t-$direction. It would seem natural to replace (6) by the difference equation

$$u_j^{n+1} = u_j^n - \frac{\lambda}{2}\left[f(u_{j+1}^n) - f(u_{j-1}^n)\right],$$

where $\lambda = \Delta t/\Delta x$ and u_j^n approximates $U(j\Delta x, n\Delta t)$. But this is known to be inappropriate because of the high degree of instability of this scheme. Replacing u_j^n by the average of its two neighbors $u_{j\pm1}^n$ we encounter the celebrated Lax-Friedrichs (LxF) scheme

$$u_j^{n+1} = \frac{u_{j+1}^n + u_{j-1}^n}{2} - \frac{\lambda}{2}\left[f(u_{j+1}^n) - f(u_{j-1}^n)\right]. \tag{7}$$

One noticeable feature of this scheme is that information on grids $j+n = even$ is independent of that on grids $j+n = odd$. Rewriting (7) gives

$$\frac{u_j^{n+1} - u_j^n}{\Delta t} + \frac{1}{2\Delta x}\left[f(u_{j+1}^n) - f(u_{j-1}^n)\right] = \frac{\frac{u_{j+1}^n + u_{j-1}^n}{2} - u_j^n}{\Delta t}. \tag{8}$$

If we denote the solution at even (or odd) grid points as u and those at odd (or even) girds as v, and bring in a scale parameter $\epsilon \sim \Delta t$, then

$$\frac{u_j^{n+1} - u_j^n}{\Delta t} + \frac{1}{2\Delta x}\left[f(v_{j+1}^n) - f(v_{j-1}^n)\right] = \frac{\frac{v_{j+1}^n + v_{j-1}^n}{2} - u_j^n}{\epsilon}. \tag{9}$$

Passing to the limit $\Delta x, \Delta t \to 0$ in (9) and keeping the parameter ϵ unchanged, we obtain a coupled system for both u and v, which in multi-dimensional case can be expressed as

$$\partial_t u + \nabla_x \cdot f(v) = \frac{1}{\epsilon}(v-u), \quad x \in \mathbb{R}^d, \quad t > 0, \tag{10}$$

$$\partial_t v + \nabla_x \cdot f(u) = \frac{1}{\epsilon}(u-v). \tag{11}$$

The main feature of this model for the system of conservation laws (6) is its high accuracy. The convergence for scalar conservation laws with general smooth flux function in arbitrary spatial dimension $\mathbb{R}^d$ is given in ([40]), and summarized in the following.

Theorem 2.1. *For any $(u_0, v_0) \in L^1(\mathbb{R}^d) \cap L^\infty(\mathbb{R}^d)$ and each fixed ϵ, let (10)–(11) admit a unique weak solution (u^ϵ, v^ϵ) on $\mathbb{R}^d \times \mathbb{R}^+$ such that $(u^\epsilon, v^\epsilon) \in C([0,\infty); L^1(\mathbb{R}^d))$, then there exists a bounded measurable function $U(x,t)$ on $\mathbb{R}^d \times \mathbb{R}^+$ such that as $\epsilon \downarrow 0$*

$$u^\epsilon \to U(x,t), \quad u^\epsilon - v^\epsilon \to 0 \quad (x,t) \in \mathbb{R}^d \times \mathbb{R}^+.$$

Moreover, U is the entropy solution of (6) with initial data $U_0(x) = \frac{1}{2}(u_0(x) + v_0(x))$ for $x \in \mathbb{R}^d$.

Corollary 2.2. *Let U be the entropy solution of the scalar conservation laws (6) with initial data $U_0 \in L^1(\mathbb{R}^d) \cap L^\infty(\mathbb{R}^d)$, and (u^ϵ, v^ϵ) be the weak solution to (10)–(11) subject to initial data with $(u_0, v_0) \in L^\infty(\mathbb{R}^d)$. Then it holds*

$$\|u^\epsilon - v^\epsilon\|_{L^1(\mathbb{R}^d)} \le \|u_0 - v_0\|_{L^1(\mathbb{R}^d)} e^{-4t/\epsilon}.$$

Furthermore,
(i) if $u_0 + v_0 = 2U_0$, then

$$\lim_{t/\epsilon \to \infty} \|u^\epsilon(\cdot,t) - U(\cdot,t)\|_{L^1(\mathbb{R}^d)} = \lim_{t/\epsilon \to \infty} \|v^\epsilon(\cdot,t) - U(\cdot,t)\|_{L^1(\mathbb{R}^d)} = 0.$$

(ii) if $u_0 = v_0 = U_0$, then

$$u^\epsilon(x,t) = v^\epsilon(x,t) = U(x,t)$$

almost everywhere in $\mathbb{R}^d \times \mathbb{R}^+$.

In an entirely similar manner, one may obtain a coupled alternating evolution system

$$\partial_t u + H(x, u, \nabla_x v) = \frac{1}{\epsilon}(v - u), \tag{12}$$

$$\partial_t v + H(x, v, \nabla_x u) = \frac{1}{\epsilon}(u - v), \tag{13}$$

as a refinement of the Hamilton-Jacobi equation

$$\partial_t \phi + H(x, \phi, \nabla_x \phi) = 0. \tag{14}$$

Based on this AE system, both high resolution finite difference method and the discontinuous Galerkin method are designed for solving the Hamilton-Jacobi equation.

3. Finite volume schemes – hyperbolic conservation laws

Consider the system of hyperbolic conservation laws

$$\partial_t u + \nabla_x \cdot f(u) = 0, \quad (x, t) \in \mathbb{R}^d \times (0, \infty), \tag{15}$$

where $u = (u_1, \ldots, u_m)^T$. In multi-dimensional case, for simplicity, we take uniform distributed grids at x_α with multi-index $\alpha = (\alpha_1, \ldots, \alpha_d)$. Let I_α be a rectangle with vertices at $\{x_{\alpha+\beta},\ |\beta| = 1\}$, labeled as $x_{\alpha\pm1}$, the number of which amounts to 2^d.

We take the average of the AE equation,

$$\partial_t u + \nabla_x \cdot f(v) = \frac{1}{\epsilon}(v - u),$$

over I_α to obtain

$$\frac{d}{dt}\bar{u}_\alpha + \frac{1}{\epsilon}\bar{u}_\alpha = \frac{1}{\epsilon}L_\alpha[v](t),$$

where $\bar{u}_\alpha = \frac{1}{|I_\alpha|}\int_{I_\alpha} u(x,t)dx$ and

$$L_\alpha[v] = \frac{1}{|I_\alpha|}\int_{I_\alpha} v\ dx - \frac{\epsilon}{|I_\alpha|}\int_{\partial I_\alpha} f(v)\cdot\nu_\alpha ds.$$

Here, $|I_\alpha|$ denotes the volume of I_α, ∂I_α indicates the boundary of I_α, and ν_α is the outward pointing unit normal field of the cell boundary ∂I_α. Let $\Phi_\alpha \sim \bar{u}_\alpha$ denote the numerical solution, and $p_\alpha[\Phi]$ a reconstructed non-

oscillatory polynomials $p_\alpha[\Phi]$ over I_α from available averages Φ_α, then we obtain a semi-discrete scheme

$$\frac{d}{dt}\Phi_\alpha + \frac{1}{\epsilon}\Phi_\alpha = \frac{1}{\epsilon}L_\alpha[\Phi], \tag{16}$$

where $p_\alpha^{SN}[\Phi]$'s constructed over neighboring cells $I_{\alpha\pm1}$ are to be used to evaluate

$$L_\alpha[\Phi] = \sum \frac{1}{|I_\alpha|}\int_{I_\alpha\cap I_{\alpha\pm1}} p_\alpha^{SN}[\Phi](x)\,dx - \sum \frac{1}{|I_\alpha|}\int_{\partial I_\alpha\cap I_{\alpha\pm1}} f(p_\alpha^{SN}[\Phi](x))\cdot ds. \tag{17}$$

Finally, in order to obtain the same order of accuracy in time, the semi-discrete scheme (16)–(17) is to be solved with an ODE solver with matching accuracy in time discretization. The evolution parameter is chosen such that

$$\epsilon\sum_{j=1}^{d}\frac{\max|f_j'(\cdot)|}{\Delta x_j} \le Q, \quad \Delta t < \epsilon, \tag{18}$$

where $Q \le 1$ depends on the order of the scheme, see (23) or (31) later in this section. For system case, $f_j's$ need to be replaced by the dominant eigenvalues over a Riemann curve.

For the 2D setting, we illustrate the corresponding AE scheme for

$$\partial_t\phi + f(\phi)_x + g(\phi)_y = 0. \tag{19}$$

3.1. First order scheme

If the reconstructed polynomial is piecewise constant, then we obtain the first order scheme as

$$\Phi_{k,l}^{n+1} = (1-\kappa)\Phi_{k,l}^n + \kappa L_{k,l}[\Phi^n], \tag{20}$$

where upon a direct calculation using $p_{k,l}[\Phi^n] = \sum \Phi_{k,l}^n\,\chi_{I_{kl}}(x,y)$, where $\chi_{I_{kl}}$ is the characteristic function which takes value one on the rectangle $I_{k,l}$, $L_{k,l}[\Phi^n]$ can be expressed as

$$\begin{aligned} L_{k,l}[\Phi^n] = A_xA_y\Phi_{k,l}^n &- \frac{\epsilon}{4\Delta x}\left(f(\Phi_{k+1,l-1}^n)\right. \\ &\left. - f(\Phi_{k-1,l-1}^n) + f(\Phi_{k+1,l+1}^n) - f(\Phi_{k-1,l+1}^n)\right) \\ &- \frac{\epsilon}{4\Delta y}\left(g(\Phi_{k-1,l+1}^n) - g(\Phi_{k-1,l-1}^n) + g(\Phi_{k+1,l+1}^n) - g(\Phi_{k+1,l-1}^n)\right), \end{aligned} \tag{21}$$

with $\kappa = \frac{\Delta t}{\epsilon}$, where A_x and A_y are the average operators in both $x-$ and $y-$ direction, respectively, so that

$$A_x A_y \Phi^n_{k,l} := \frac{1}{4}\left(\Phi^n_{k-1,l-1} + \Phi^n_{k+1,l-1} + \Phi^n_{k+1,l+1} + \Phi^n_{k-1,l+1}\right). \tag{22}$$

The parameter ϵ is chosen so that

$$\epsilon\left(\frac{\max|f'|}{\Delta x} + \frac{\max|g'|}{\Delta y}\right) \leq 1 \quad \text{and} \quad \Delta t \ < \ \epsilon, \tag{23}$$

which ensures the scalar maximum principle

$$|\Phi^{n+1}|_\infty \ \leq \ |\Phi^n|_\infty, \quad n \in \mathbb{N}. \tag{24}$$

Again, for system case, both $|f'|$ and $|g'|$ in the stability requirement (23) needs to be replaced by dominant eigenvalues of the corresponding Jacobian matrices.

3.2. Second order scheme

The second order scheme requires a linear polynomial reconstruction, its formulation in the rectangle $I_{kl} = [x_k - \Delta x, x_k + \Delta x] \times [y_k - \Delta y, y_k + \Delta y]$ has the form

$$p_{k,l}[\Phi^n](x,y) \ = \ \sum_{k,l}\left(\Phi^n_{k,l} + s'_{k,l}(x - x_k) + s\backprime_{k,l}(y - y_l)\right)\chi_{I_{kl}}(x,y), \tag{25}$$

where s' and $s\backprime$ are the numerical derivatives corresponding to Φ_x and Φ_y. Now, using the midpoint quadrature rule in evaluation of (17), we obtain the second order AE scheme

$$\frac{d}{dt}\Phi_{k,l} = L_{k,l}[\Phi]$$

with

$$\begin{aligned} L_{k,l}[\Phi] = A_x A_y \Phi_{k,l} &+ \frac{\Delta x}{8}\left(s'_{k-1,l-1} - s'_{k+1,l-1} - s'_{k+1,l+1} + s'_{k-1,l+1}\right) \\ &+ \frac{\Delta y}{8}\left(s\backprime_{k-1,l-1} + s\backprime_{k+1,l-1} - s\backprime_{k+1,l+1} - s\backprime_{k-1,l+1}\right) \\ &- \frac{\epsilon}{4\Delta x}\left[f\left(\Phi_{k+1,l-1} + \frac{\Delta y}{2}s\backprime_{k+1,l-1}\right) - f\left(\Phi_{k-1,l-1} + \frac{\Delta y}{2}s\backprime_{k-1,l-1}\right)\right. \end{aligned}$$

$$+ f\left(\Phi_{k+1,l+1} - \frac{\Delta y}{2} s_{k+1,l+1}^{\backprime}\right) - f\left(\Phi_{k-1,l+1} - \frac{\Delta y}{2} s_{k-1,l+1}^{\backprime}\right)\Bigg]$$
$$- \frac{\epsilon}{4\Delta y}\Bigg[g\left(\Phi_{k-1,l+1} + \frac{\Delta x}{2} s'_{k-1,l+1}\right) - g\left(\Phi_{k-1,l-1} + \frac{\Delta x}{2} s'_{k-1,l-1}\right)$$
$$+ g\left(\Phi_{k+1,l+1} - \frac{\Delta x}{2} s'_{k+1,l+1}\right) - g\left(\Phi_{k+1,l-1} - \frac{\Delta x}{2} s'_{k+1,l-1}\right)\Bigg].$$

The non-oscillatory property requires that we choose $s'_{k,l}$ and $s_{k,l}^{\backprime}$ with certain limiters. In [41] the basic minmod limiter is adopted:

$$s'_{k,l} = minmod\left\{\frac{\Phi^n_{k+2,l} - \Phi^n_{k,l}}{2\Delta x}, \frac{\Phi^n_{k,l} - \Phi^n_{k-2,l}}{2\Delta x}\right\}, \tag{26}$$

$$s_{k,l}^{\backprime} = minmod\left\{\frac{\Phi^n_{k,l+2} - \Phi^n_{k,l}}{2\Delta y}, \frac{\Phi^n_{k,l} - \Phi^n_{k,l-2}}{2\Delta y}\right\}, \tag{27}$$

with

$$minmod\{a_1, a_2, \ldots\} = \begin{cases} \min\limits_i\{a_i\} & \text{if } a_i > 0 \ \forall i, \\ \max\limits_i\{a_i\} & \text{if } a_i < 0 \ \forall i, \\ 0 & \text{otherwise.} \end{cases} \tag{28}$$

When the second order Runge-Kutta time discretization is used, the scheme becomes

$$\Phi^*_{k,l} = (1-\kappa)\Phi^n_{k,l} + \kappa L_{k,l}[\Phi^n], \tag{29}$$

$$\Phi^{n+1}_{k,l} = \frac{1}{2}\Phi^n_{k,l} + \frac{1}{2}(1-\kappa)\Phi^*_{k,l} + \frac{\kappa}{2} L_{k,l}[\Phi^*]. \tag{30}$$

Indeed analysis in [41] shows that such a choice again yields the scalar maximum principle (24), provided

$$\epsilon\left(\frac{\max|f'|}{\Delta x} + \frac{\max|g'|}{\Delta y}\right) \le \frac{1}{4} \quad \text{and} \quad \Delta t < \epsilon. \tag{31}$$

Even higher order schemes can be constructed using the ENO selection of more stencils, see [41] for further details.

4. Finite difference schemes – Hamilton-Jacobi equations

To approximate the multi-dimensional HJ equations:

$$\partial_t \phi + H(x, \nabla_x \phi) = 0, \quad x \in \mathbb{R}^d,$$

we start with the AE formulation

$$\partial_t u + \frac{1}{\epsilon} u = \frac{1}{\epsilon} v - H(x, \nabla_x v). \tag{32}$$

Again we use $\{x_\alpha\}$ to denote uniformly distributed grids in $\mathbb{R}^d$, and I_α as a hypercube centered at x_α with vertices at $x_{\alpha\pm 1}$ where the number of vertices is 2^d.

In [42] we present two different constructions of AE schemes for multi-dimensions. For the first type, given grid values $\{\Phi_\alpha\}$, we construct a continuous, piecewise polynomial $p_\alpha[\Phi](x) \in P_r$ defined in I_α such that

$$p_\alpha[\Phi](x_{\alpha\pm 1}) = \Phi_{\alpha\pm 1}.$$

Here P_r denotes a linear space of all polynomials of degree at most r in all x_i:

$$P_r := \{p \mid p(x) = \sum_{0\le\beta_i\le r} a_\beta (x - x_\alpha)^\beta, \quad 1 \le i \le d, \quad a_\beta \in \mathbb{R}\}.$$

Sampling the AE system (32) at x_α, which is the common vertex of $I_{\alpha\pm 1}$, while using these polynomials on the right hand side of (32), we obtain the semi-discrete AE scheme

$$\begin{aligned} \frac{d}{dt}\Phi_\alpha + \frac{1}{\epsilon}\Phi_\alpha &= \frac{1}{\epsilon} L_\alpha[\Phi], \\ L_\alpha[\Phi] &= p_\alpha^{SN}[\Phi](x_\alpha) - \epsilon H(x_\alpha, \nabla_x p_\alpha^{SN}[\Phi](x_\alpha)), \end{aligned} \tag{33}$$

where $p_\alpha^{SN}[\Phi]$'s are constructed using neighboring grid values. Using this sampling approach, construction of schemes of higher than second order will become cumbersome.

In [42] we presented a simpler approach of reconstruction, called the dimension-by-dimension approach. Such an approach can be easily derived for higher order schemes, and work equally well with hyperbolic conservation laws. We illustrate the approach in the two dimensional setting.

We construct interpolated polynomials, $p_{j,k}$ and $q_{j,k}$ in the $x-$ and $y-$ direction as in one-dimensional case, satisfying

$$\begin{aligned} p_{j,k}[\Phi](x_{j\pm 1}, y_k) &= \Phi_{j\pm 1,k}, \\ q_{j,k}[\Phi](x_j, y_{k\pm 1}) &= \Phi_{j,y\pm 1}, \end{aligned}$$

so that for Hamiltonian $H = H(\nabla_x \phi)$ we have

$$L_{j,k} = \frac{p_{j,k}[\Phi](x_j, y_k) + q_{j,k}[\Phi](x_j, y_k)}{2} - \epsilon H\left(\partial_x p_{j,k}[\Phi](x_j, y_k), \partial_y q_{j,k}[\Phi](x_j, y_k)\right). \tag{34}$$

4.1. First order scheme

For the first order scheme, such an interpolant is given by

$$\begin{aligned} p^1_{j,k}[\Phi](x,y) &= \Phi_{j-1,k} + s^x_{j,k}(x - x_{j-1}), \\ q^1_{j,k}[\Phi](x,y) &= \Phi_{j,k-1} + s^y_{j,k}(y - y_{k-1}), \end{aligned}$$

where

$$s^x_{j,k} = \frac{\Phi_{j+1,k} - \Phi_{j-1,k}}{2\Delta x}, \qquad s^y_{j,k} = \frac{\Phi_{j,k+1} - \Phi_{j,k-1}}{2\Delta y}.$$

Evaluating at the polynomials and their partial derivatives at (x_j, y_k) yields

$$\begin{aligned} p^1_{j,k}[\Phi](x_j, y_k) &= \frac{\Phi_{j+1,k} + \Phi_{j-1,k}}{2}, \qquad \partial_x p^1_{j,k}[\Phi](x_j, y_k) = s^x_{j,k}, \\ q^1_{j,k}[\Phi](x_j, y_k) &= \frac{\Phi_{j,k+1} + \Phi_{j,k-1}}{2}, \qquad \partial_y q^1_{j,k}[\Phi](x_j, y_k) = s^y_{j,k}. \end{aligned}$$

Substituting this into (34) yields

$$L_{j,k}[\Phi] = A_x A_y \Phi_{j,k} - \epsilon H(s^x_{j,k}, s^y_{j,k}) \tag{35}$$

so that

$$\Phi^{n+1}_{j,k} = (1 - \kappa)\Phi^n_{j,k} + \kappa L_{j,k}[\Phi^n].$$

4.2. Second order scheme

For the second order scheme, the continuous, piecewise interpolating polynomial is given by

$$\begin{aligned} p^2_{j,k}[\Phi](x,y) &= \Phi_{j-1,k} + s^x_{j,k}(x - x_{j-1}) + \frac{(s^x_{j,k})'}{2}(x - x_{j-1})(x - x_{j+1}), \\ q^2_{j,k}[\Phi](x,y) &= \Phi_{j,k-1} + s^y_{j,k}(y - y_{j-1}) + \frac{(s^y_{j,k})'}{2}(y - y_{k-1})(y - y_{k+1}), \end{aligned}$$

where the approximations to the send order derivative are selected using the ENO interpolation technique,

$$\begin{aligned}(s^x_{j,k})' &= M\left\{\frac{s^x_{j+2,k}-s^x_{j,k}}{2\Delta x},\frac{s^x_{j,k}-s^x_{j-2,k}}{2\Delta x}\right\},\\ (s^y_{j,k})' &= M\left\{\frac{s^y_{j,k+2}-s^y_{j,k}}{2\Delta y},\frac{s^y_{j,k}-s^y_{j,k-2}}{2\Delta y}\right\},\end{aligned}$$

where $M\{a,b\}=a$ if $|a|\le|b|$, $M\{a,b\}=b$ otherwise. We then obtain

$$\begin{aligned}p^2_{j,k}[\Phi](x_j,y_k) &= \frac{\Phi_{j+1,k}+\Phi_{j-1,k}}{2}-\frac{(s^x_{j,k})'}{2}(\Delta x)^2, \quad \partial_x p^2_{j,k}[\Phi](x_j,y_k)=s^x_{j,k},\\ q^2_{j,k}[\Phi](x_j,y_k) &= \frac{\Phi_{j,k+1}+\Phi_{j,k-1}}{2}-\frac{(s^y_{j,k})'}{2}(\Delta y)^2, \quad \partial_y q^2_{j,k}[\Phi](x_j,y_k)=s^y_{j,k}.\end{aligned}$$

so that

$$L_{j,k}[\Phi]=A_xA_y\Phi_{j,k}-\frac{(s^x_{j,k})'}{2}(\Delta x)^2-\frac{(s^y_{j,k})'}{2}(\Delta y)^2-\epsilon H(s^x_{j,k},s^y_{j,k}).$$

Combining with a second order Runge-Kutta method gives,

$$\begin{aligned}\Phi^*_{j,k} &= (1-\kappa)\Phi^n_{j,k}+\kappa L_{j,k}[\Phi^n],\\ \Phi^{n+1}_{j,k} &= \frac{1}{2}\Phi^n_{j,k}+\frac{1-\kappa}{2}\Phi^*_{j,k}+\frac{\kappa}{2}L_{j,k}[\Phi^*].\end{aligned}$$

4.3. Third order scheme

The third order scheme formulation is based on the following cubic polynomials

$$\begin{aligned}p^3_{j,k}[\Phi](x,y) &= p^2_{j,k}[\Phi](x,y)+\frac{(s^x_{j,k})''}{6}(x-x_{j-1})(x-x_{j+1})(x-x^*),\\ q^3_{j,k}[\Phi](x,y) &= q^2_{j,k}[\Phi](x,y)+\frac{(s^y_{j,k})''}{6}(y-y_{k-1})(y-y_{k+1})(y-y^*),\end{aligned}$$

where

$$(s^x_{j,k})'' = M\left\{\frac{(s^x_{j+2,k})'-(s^x_{j,k})'}{2\Delta x},\frac{(s^x_{j,k})'-(s^x_{j-2,k})'}{2\Delta x}\right\},$$

$$(s^y_{j,k})'' = M\left\{\frac{(s^y_{j,k+2})' - (s^y_{j,k})'}{2\Delta y}, \frac{(s^y_{j,k})' - (s^y_{j,k-2})'}{2\Delta y}\right\}.$$

Here x^* is chosen as the grid point value used in the ENO procedure for $(s^x_{j,k})'$ so that $x^* = x_{j-3}$ or $x^* = x_{j+3}$. The value y^* is chosen in a similar way. This gives

$$\begin{aligned}
p^3_{j,k}[\Phi](x_j, y_k) &= \frac{\Phi_{j+1,k} + \Phi_{j-1,k}}{2} - \frac{(s^x_{j,k})'}{2}(\Delta x)^2 - \frac{(s^x_{j,k})''}{6}(\Delta x)^2(x_j - x^*),\\
\partial_x p^3_{j,k} &= s^x_{j,k} - \frac{(s^x_{j,k})''}{6}(\Delta x)^2,\\
q^3_{j,k}[\Phi](x_j, y_k) &= \frac{\Phi_{j,k+1} + \Phi_{j,k-1}}{2} - \frac{(s^y_{j,k})'}{2}(\Delta y)^2 - \frac{(s^y_{j,k})''}{6}(\Delta y)^2(y_k - y^*),\\
\partial_y q^3_{j,k} &= s^y_{j,k} - \frac{(s^y_{j,k})''}{6}(\Delta y)^2.
\end{aligned}$$

When combined with the third order Runge-Kutta method, this gives

$$\begin{aligned}
\Phi^{(1)}_{j,k} &= (1-\kappa)\Phi^n_{j,k} + \kappa L_{j,k}[\Phi^n],\\
\Phi^{(2)}_{j,k} &= \frac{3}{4}\Phi^n_{j,k} + \frac{1}{4}(1-\kappa)\Phi^{(1)}_{j,k} + \frac{1}{4}\kappa L_{j,k}[\Phi^{(1)}],\\
\Phi^{n+1}_{j,k} &= \frac{1}{3}\Phi^n_{j,k} + \frac{2}{3}(1-\kappa)\Phi^{(2)}_{j,k} + \frac{2}{3}\kappa L_{j,k}[\Phi^{(2)}],
\end{aligned}$$

where

$$\begin{aligned}
L_{j,k}[\Phi] &= A_x A_y \Phi_{j,k} - \frac{(s^x_{j,k})'}{2}(\Delta x)^2 - \frac{(s^y_{j,k})'}{2}(\Delta y)^2\\
&\quad - \frac{(s^x_{j,k})''}{6}(\Delta x)^2(x - x^*) - \frac{(s^y_{j,k})''}{6}(\Delta y)^2(y - y^*)\\
&\quad - \epsilon H\left(s^x_{j,k} - \frac{(s^x_{j,k})''}{6}(\Delta x)^2, s^y_{j,k} - \frac{(s^y_{j,k})''}{6}(\Delta y)^2\right).
\end{aligned}$$

We remark that this scheme can be easily derived for higher orders using an ENO procedure for derivative approximations.

5. Discontinuous Galerkin schemes

We begin to formulate discontinuous Galerkin schemes in one dimensional setting. Let the spatial domain be divided to form a uniform grid $\{x_j\}$,

with $\Delta x = x_{j+1} - x_j$. We denote $I_j = (x_{j-1}, x_{j+1})$ for $j = 2, \ldots, N-1$ with $I_1 = (x_1, x_2)$ and $I_N = (x_{N-1}, x_N)$. Centered at each grid $\{x_j\}$, the numerical approximation is a polynomial $\Phi|_{I_j} = \Phi_j(x) \in P^k$, where P^k denotes a linear space of all polynomials of degree at most k:

$$P^k := \{p \,|\, p(x)|_{I_j} = \sum_{0 \le i \le k} a_i (x - x_j)^i, \quad a_i \in \mathbb{R}\}.$$

Note $\dim(P^k) = k+1$. We denote $v(x^\pm) = \lim_{\epsilon \to 0\pm} v(x+\epsilon)$, and $v_j^\pm = v(x_j^\pm)$. The jump at x_j is $[v]_j = v(x_j^+) - v(x_j^-)$, and the average $\{v\}_j = \frac{1}{2}(v_j^+ + v_j^-)$.

5.1. The Hamilton-Jacobi equation

We start with the one-dimensional Hamilton-Jacobi equation of the form

$$\partial_t \phi + H(x, \phi, \phi_x) = 0.$$

Again the 'building base' is the following AE formulation

$$\partial_t u + H(x, u, v_x) = \frac{1}{\epsilon}(v - u). \tag{36}$$

Integrating (36) over I_j against the test function $\eta \in P^k(I_j)$, we obtain the semi-discrete AEDG scheme

$$\begin{aligned} &\int_{I_j} (\partial_t \Phi_j + H(x, \Phi_j, \partial_x \Phi_j^{SN}))\eta dx + \lambda [\Phi_j^{SN}]\Big|_{x_j} \eta(x_j) \\ &\quad = \frac{1}{\epsilon}\left(\int_{I_j} \Phi_j^{SN} \eta dx - \int_{I_j} \Phi_j \eta dx \right), \end{aligned} \tag{37}$$

where $\lambda = H_p(x_j, \Phi_j(x_j), \partial_x \Phi_j(x_j))$ and Φ_j^{SN} is sampled from neighboring polynomials $\Phi_{j\pm1}$ in the following way:

$$\begin{aligned} \int_{I_j} H(x, \Phi_j, \partial_x \Phi_j^{SN})\eta dx &= \int_{x_{j-1}}^{x_j} H(x, \Phi_j, \partial_x \Phi_{j-1})\eta dx \\ &\quad + \int_{x_j}^{x_{j+1}} H(x, \Phi_j, \partial_x \Phi_{j+1})\eta dx, \\ \int_{I_j} \Phi_j^{SN} \eta dx &= \int_{x_{j-1}}^{x_j} \Phi_{j-1} \eta dx + \int_{x_j}^{x_{j+1}} \Phi_{j+1} \eta dx, \\ [\Phi_j^{SN}]\Big|_{x_j} &= \Phi_{j+1}(x_j^+) - \Phi_{j-1}(x_j^-). \end{aligned}$$

To update each grid-centered polynomial element Φ, we write the compact form of the semi-discrete scheme

$$\frac{d}{dt}\int_{I_j}\Phi_j\eta dx = L[\Phi_j;\Phi_j^{SN},\eta](t), \tag{38}$$

where

$$\begin{aligned} L[\Phi_j;\Phi_{j\pm1},\eta](t) = &\frac{1}{\epsilon}\int_{I_j}(\Phi_j^{SN}-\Phi_j)\eta dx \\ &-\int_{I_j}H\left(x,\Phi_j,\partial_x\Phi_j^{SN}\right)\eta dx - \lambda[\Phi_j^{SN}]|_{x_j}\eta(x_j). \end{aligned} \tag{39}$$

We use boundary cells I_1 and I_N to incorporate proper boundary condtions. For a computational domain $[a,b]$ with $x_1 = a, x_N = b$ and $\Delta x = (b-a)/(N-1)$, the equations in two end cells may be given as

$$\begin{aligned} &\int_{x_1}^{x_2}(\partial_t\Phi_1 + H(x,\Phi_1,\partial_x\Phi_2))\eta dx + \frac{\lambda}{2}[\Phi]|_{x_1}\eta(x_1) \\ &\quad = \frac{1}{\epsilon}\int_{x_1}^{x_2}(\Phi_2-\Phi_1)\eta dx, \end{aligned} \tag{40}$$

$$\begin{aligned} &\int_{x_{N-1}}^{x_N}(\partial_t\Phi_N + H(x,\Phi_N,\partial_x\Phi_{N-1}))\eta dx + \frac{\lambda}{2}[\Phi]|_{x_N}\eta(x_N) \\ &\quad = \frac{1}{\epsilon}\int_{x_{N-1}}^{x_N}(\Phi_{N-1}-\Phi_N)\eta dx. \end{aligned} \tag{41}$$

If the flow is incoming at $x = a$, one has to impose a boundary condition $\phi(a,t) = g_1(t)$. As a result, one is required to modify (40) by changing $[\Phi]$ to $\Phi_2(x_1^+) - g_1(t)$; for the outflow case, one may take $[\Phi] = 0$ in (40). Similarly, at $x = b$, the inflow boundary condition $\phi(b,t) = g_2(t)$ can be incorporated in (41) by replacing $[\Phi]$ by $g_2(t) - \Phi_{N-1}(x_N^-,t)$; and for outgoing flow, replacing $[\Phi]$ by 0. The determination of the inflow or outflow of the boundary condition may be obtained by checking the sign of the characteristic speed $\partial_x H(x,\phi,p)$. In the case of periodic boundary conditions, $[\Phi]$ can be computed as $\Phi_2(x_1^+) - \Phi_{N-1}(x_N^-)$ at $x = x_1, x_N$, and $\Phi_N(x)$ is regarded to be identical to $\Phi_1(x)$.

The fully discrete scheme follows from applying an appropriate Runge-Kutta solver to (38). We summarize the algorithm as follows.

Algorithm:

1. Initialization: in any cell I_j, compute the initial data by the local L^2-projection

$$\int_{I_j} (\Phi^0 - \phi_0)\eta dx = 0, \quad \eta \in P^k(I_j). \tag{42}$$

2. Alternating evaluation: take polynomials $\Phi_{j\pm1}(x) = \Phi|_{I_{j\pm1}}$, and then sample in I_j to get $L[\Phi_j; \Phi_{j\pm1}, \eta]$ as defined in (39).
3. Evolution: obtain Φ^{n+1} from Φ^n by some Runge-Kutta type procedure to solve the ODE system (38).

In the AEDG schemes, ϵ is chosen such that the stability condition,

$$\Delta t \le \epsilon \le Q \frac{\Delta x}{\max |H_p(x, \phi, p)|},$$

is satisfied. The choice of Q depends on the order of the scheme.

The semi-discrete AEDG scheme is shown to be L^2-stable for linear Hamiltonian. In particular, when $H = \alpha p,\ \alpha = const.$, we have the following (see [42]).

Theorem 5.1. *Let Φ be computed from the AEDG scheme (38) for the Hamilton-Jacobi equation $\partial_t\phi + H(\partial_x\phi) = 0$ with linear Hamiltonian $H(p) = \alpha p$ and periodic boundary conditions. Then*

$$\frac{d}{dt}\int_a^b \Phi^2 dx = -\frac{1}{\epsilon}\int_a^b (u - v)^2 dx.$$

By similar procedures one can construct AEDG schemes for multi-dimensional H-J equations:

$$\partial_t\phi + H(\nabla_x\phi) = 0, \quad x := (x^1, \ldots, x^d) \in \mathbb{R}^d,$$

based on the AE formulation (32). Let $\{x_\alpha\}$ be distributed grids in $\mathbb{R}^d$, and I_α be a hypercube centered at x_α with vertices at $x_{\alpha\pm1}$. Centered at each grid $\{x_\alpha\}$, the numerical approximation is a polynomial $\Phi|_{I_\alpha} = \Phi_\alpha(x) \in P_r$, where P_r denotes a linear space of all polynomials of degree at most r in all x_i:

$$P_r := \{p \mid p(x)|_{I_\alpha} = \sum_{0\le\beta_i\le r} a_\beta (x - x_\alpha)^\beta, \quad 1 \le i \le d, \quad a_\beta \in \mathbb{R}\}.$$

Note $\dim(P_r) = (r+1)^d$. Integrating the AE system (32) over I_α against the test function $\eta \in P_r$, we obtain the semi-discrete AEDG scheme

$$\int_{I_\alpha} (\partial_t \Phi_\alpha + H(\nabla_x \Phi_\alpha^{SN}))\eta dx + \frac{1}{\epsilon}\int_{I_\alpha} \Phi_\alpha \eta dx = \frac{1}{\epsilon}\int_{I_\alpha} \Phi_\alpha^{SN}\eta dx - B, \tag{43}$$

$$B = \sum_{j=1}^{d} \int_{I_\alpha} H_j(\nabla \Phi_\alpha^{SN})[\Phi_\alpha^{SN}]\eta(x)\delta(x^j - x_{\alpha_j}^j)dx, \tag{44}$$

where Φ_α^{SN} is sampled from neighboring polynomials, and $H_j = \partial_{p_j} H(p)$. The choice of Φ_α^{SN} is not unique, and we shall take

$$\Phi_\alpha^{SN} \in \text{span}\{\Phi_{\alpha \pm e_j}\}_{j=1}^d.$$

We next illustrate our options in the two dimensional case. For $\alpha = (i, j)$, the terms involving neighboring polynomials are as follows:

$$\begin{aligned}
&\int_{x_{i-1}}^{x_{i+1}} \int_{y_{j-1}}^{y_{j+1}} H(\partial_x \Phi^{SN}, \partial_y \Phi^{SN})\eta dy dx \\
&= \int_{x_i}^{x_{i+1}} \int_{y_j}^{y_{j+1}} H(\partial_x \Phi_{i+1,j}, \partial_y \Phi_{i,j+1})\eta(x,y) dy dx \\
&\quad + \int_{x_i}^{x_{i+1}} \int_{y_{j-1}}^{y_j} H(\partial_x \Phi_{i+1,j}, \partial_y \Phi_{i,j-1})\eta(x,y) dy dx \\
&\quad + \int_{x_{i-1}}^{x_i} \int_{y_j}^{y_{j+1}} H(\partial_x \Phi_{i-1,j}, \partial_y \Phi_{i,j+1})\eta(x,y) dy dx \\
&\quad + \int_{x_{i-1}}^{x_i} \int_{y_{j-1}}^{y_j} H(\partial_x \Phi_{i-1,j}, \partial_y \Phi_{i,j-1})\eta(x,y) dy dx.
\end{aligned}$$

An average of two neighboring polynomials $\Phi_{i\pm1,j}$ and $\Phi_{i,j\pm1}$ will be used to evaluate $\int_{I_\alpha} \Phi^{SN}\eta dx$, that is

$$\begin{aligned}
\int_{I_\alpha} \Phi^{SN}\eta dx &= \frac{1}{2}\int_{x_i}^{x_{i+1}} \int_{y_j}^{y_{j+1}} (\Phi_{i+1,j} + \Phi_{i,j+1})\eta(x,y) dy dx \\
&\quad + \frac{1}{2}\int_{x_i}^{x_{i+1}} \int_{y_{j-1}}^{y_j} (\Phi_{i+1,j} + \Phi_{i,j-1})\eta(x,y) dy dx \\
&\quad + \frac{1}{2}\int_{x_{i-1}}^{x_i} \int_{y_j}^{y_{j+1}} (\Phi_{i-1,j} + \Phi_{i,j+1})\eta(x,y) dy dx \\
&\quad + \frac{1}{2}\int_{x_{i-1}}^{x_i} \int_{y_{j-1}}^{y_j} (\Phi_{i-1,j} + \Phi_{i,j-1})\eta(x,y) dy dx.
\end{aligned}$$

The B term in (44) can then be computed as

$$\begin{aligned} B &= \int_{y_{j-1}}^{y_{j+1}} H_1\left(\partial_x\Phi_{i,j}, \partial_y\Phi_{i,j}\right)\left(\Phi_{i+1,j}(x_i^+, y) - \Phi_{i-1,j}(x_i^-, y)\right)\eta(x_i, y)dy \\ &+ \int_{x_{i-1}}^{x_{i+1}} H_2\left(\partial_x\Phi_{i,j}, \partial_y\Phi_{i,j}\right)\left(\Phi_{i,j+1}(x, y_j^+) - \Phi_{i,j-1}(x, y_j^-)\right)\eta(x, y_j)dx. \end{aligned}$$

For the boundaries, we first consider the side boundary along $x = x_1$. Then

$$\begin{aligned} &\int_{x_1}^{x_2}\int_{y_{j-1}}^{y_{j+1}} H(\partial_x\Phi^{SN}, \partial_y\Phi^{SN})\eta dydx \\ &= \int_{x_1}^{x_2}\int_{y_j}^{y_{j+1}} H(\partial_x\Phi_{2,j}, \partial_y\Phi_{1,j+1})\eta(x, y)dydx \\ &\quad + \int_{x_1}^{x_2}\int_{y_{j-1}}^{y_j} H(\partial_x\Phi_{2,j}, \partial_y\Phi_{1,j-1})\eta(x, y)dydx, \end{aligned}$$

and

$$\begin{aligned} \int_{x_1}^{x_2}\int_{y_{j-1}}^{y_{j+1}} \Phi^{SN}\eta dydx &= \frac{1}{2}\int_{x_1}^{x_2}\int_{y_j}^{y_{j+1}} (\Phi_{2,j} + \Phi_{1,j+1})\eta(x, y)dydx \\ &\quad + \frac{1}{2}\int_{x_1}^{x_2}\int_{y_{j-1}}^{y_j} (\Phi_{2,j} + \Phi_{1,j-1})\eta(x, y)dydx, \end{aligned}$$

and

$$\begin{aligned} B &= \frac{1}{2}\int_{y_{j-1}}^{y_{j+1}} H_1\left(\partial_x\Phi_{1,j}, \partial_y\Phi_{1,j}\right)\left(\Phi_{2,j}(x_1^+, y) - \Phi_{0,j}(x_1^-, y)\right)\eta(x_1, y)dy \\ &+ \int_{x_1}^{x_2} H_2\left(\partial_x\Phi_{1,j}, \partial_y\Phi_{1,j}\right)\left(\Phi_{1,j+1}(x, y_j^+) - \Phi_{1,j-1}(x, y_j^-)\right)\eta(x, y_j)dx. \end{aligned}$$

In the above, $\Phi_{0,j}(x_1^-, y)$ may be taken different ways: the given boundary data at x_1 for inflow boundary; $\Phi_{2,j}(x_1, y)$ for outgoing flow; and $\Phi_{N_x-1,j}(x_{N_x}^-, y)$ for periodic boundary conditions. Similar computations are made along the other side boundaries $x = x_{Nx}, y = y_1, y = y_{Ny}$.

For corner cells, we illustrate using the southwest corner (x_1, y_1):

$$\int_{x_1}^{x_2}\int_{y_1}^{y_2} H(\partial_x\Phi^{SN}, \partial_y\Phi^{SN})\eta dydx = \int_{x_1}^{x_2}\int_{y_1}^{y_2} H(\partial_x\Phi_{2,1}, \partial_y\Phi_{1,2})\eta(x, y)dydx,$$

and

$$\int_{x_1}^{x_2}\int_{y_1}^{y_2}\Phi^{SN}\eta dydx=\frac{1}{2}\int_{x_1}^{x_2}\int_{y_1}^{y_2}(\Phi_{2,1}+\Phi_{1,2})\eta(x,y)dydx,$$

and

$$\begin{aligned}B &= \frac{1}{2}\int_{y_1}^{y_2}H_1\left(\partial_x\Phi_{1,1},\partial_y\Phi_{1,1}\right)\left(\Phi_{2,1}(x_1^+,y)-\Phi_{0,1}(x_1^-,y)\right)\eta(x_1,y)dy\\ &+ \frac{1}{2}\int_{x_1}^{x_2}H_2\left(\partial_x\Phi_{1,1},\partial_y\Phi_{1,1}\right)\left(\Phi_{1,2}(x,y_1^+)-\Phi_{1,0}(x,y_1^-)\right)\eta(x,y_1)dx.\end{aligned}$$

Similar computations can be made for the other corners $(x_1,y_{Ny}),(x_{Nx},y_1)$, (x_{Nx},y_{Ny}).

Boundary conditions are incorporated in the following ways:

$$\Phi_{0,1}(x_1^-,y)=\begin{cases}\text{boundary data} & \text{inflow},\\ \Phi_{2,1}(x_1^+,y) & \text{outflow},\\ \Phi_{N_x-1,1}(x_{N_x}^-,y) & \text{periodic},\end{cases}$$

$$\Phi_{1,0}(x,y_1^-)=\begin{cases}\text{boundary data} & \text{inflow},\\ \Phi_{1,2}(x,y_1^+) & \text{outflow},\\ \Phi_{1,N_y-1}(x_1,y_{N_y}^-) & \text{periodic}.\end{cases}$$

The Runge-Kutta method is used for time discretization with matching accuracy.

5.2. Hyperbolic conservation laws

The AEDG method designed in [42] for Hamilton-Jacobi equations can be applied without any difficulty to hyperbolic conservation laws. We only outline the main idea and the scheme formulation. Again the AEDG for one dimensional conservation laws of the form $\partial_t u+\partial_x f(u)=0$ can be derived based on the AE formulation

$$\partial_t u+\partial_x f(v) = \frac{1}{\epsilon}(v-u). \tag{45}$$

Integrating the AE system (45) over I_j against the test function $\eta\in P^k(I_j)$, we obtain the semi-discrete AEDG scheme

$$\int_{I_j} (\partial_t \Phi_j + \partial_x f(\Phi_j^{SN}))\eta dx + [f(\Phi_j^{SN})]\Big|_{x_j} \eta(x_j) = \frac{1}{\epsilon}\left(\int_{I_j} \Phi_j^{SN}\eta dx - \int_{I_j} \Phi_j \eta dx\right), \tag{46}$$

where Φ_j^{SN} is sampled from neighboring polynomials $\Phi_{j\pm1}$ in the following way:

$$\begin{aligned}
\int_{I_j} \partial_x f(\Phi_j^{SN})\eta dx &= \int_{x_{j-1}}^{x_j} \partial_x f(\Phi_{j-1})\eta dx + \int_{x_j}^{x_{j+1}} \partial_x f(\Phi_{j+1})\eta dx,\\
\int_{I_j} \Phi_j^{SN}\eta dx &= \int_{x_{j-1}}^{x_j} \Phi_{j-1}\eta dx + \int_{x_j}^{x_{j+1}} \Phi_{j+1}\eta dx,\\
[f(\Phi_j^{SN})]\Big|_{x_j} &= f(\Phi_{j+1}(x_j^+)) - f(\Phi_{j-1}(x_j^-)).
\end{aligned}$$

To update each grid-centered polynomial element $\Phi_j(x)$, we write the compact form of the semi-discrete scheme

$$\frac{d}{dt}\int_{I_j} \Phi_j \eta dx = L[\Phi_j; \Phi_j^{SN}, \eta](t), \tag{47}$$

where

$$L[\Phi_j; \Phi_{j\pm1}, \eta](t) = \frac{1}{\epsilon}\int_{I_j} (\Phi_j^{SN} - \Phi_j)\eta dx - \int_{I_j} \partial_x f\left(\Phi_j^{SN}\right)\eta dx - [f(\Phi_j^{SN})]|_{x_j}\eta(x_j). \tag{48}$$

Boundary conditions are incorporated through equations in two end cells. For a computational domain $[a, b]$ with $x_1 = a, x_N = b$ and $\Delta x = (b - a)/(N - 1)$, the equations in two end cells are given by

$$\int_{x_1}^{x_2} (\partial_t \Phi_1 + \partial_x f(\Phi_2))\eta dx + \frac{1}{2}[f(\Phi)]|_{x_1}\eta(x_1) = \frac{1}{\epsilon}\int_{x_1}^{x_2} (\Phi_2 - \Phi_1)\eta dx, \tag{49}$$

$$\int_{x_{N-1}}^{x_N} (\partial_t \Phi_N + \partial_x f(\Phi_{N-1}))\eta dx + \frac{1}{2}[f(\Phi)]|_{x_N}\eta(x_N) = \frac{1}{\epsilon}\int_{x_{N-1}}^{x_N} (\Phi_{N-1} - \Phi_N)\eta dx. \tag{50}$$

If the flow is incoming at $x = a$, one needs to impose the given boundary condition $\phi(a,t) = g_1(t)$. As a consequence, one is required to modify (49) by changing $[f(\Phi)]$ to $f(\Phi_2(x_1^+)) - f(g_1(t))$; for the outflow case, one may take $[f(\Phi)] = 0$ in (49). Similarly, at $x = b$, the inflow boundary condition $\phi(b,t) = g_2(t)$ can be incorporated in (50) by replacing $[f(\Phi)]$ by $f(g_2(t)) - f(\Phi_{N-1}(x_N^-,t))$; and for outgoing flow, replacing $[f(\Phi)]$ by 0. The determination of the inflow or outflow of the boundary condition may be obtained by checking the sign of the characteristic speed $f'(u)$. In the case of periodic boundary conditions, $[f(\Phi)]$ can be computed as $f(\Phi_2(x_1^+)) - f(\Phi_{N-1}(x_N^-))$ at $x = x_1, x_N$, and $\Phi_N(x)$ is regarded to be identical to $\Phi_1(x)$.

The fully discrete scheme follows from applying an appropriate Runge-Kutta solver to (47). We summarize the algorithm as follows.

Algorithm:

1. Initialization: in any cell I_j, compute the initial data by the local L^2-projection

$$\int_{I_j} (\Phi^0 - \phi_0)\eta dx = 0, \quad \eta \in P^k(I_j). \tag{51}$$

2. Alternating evaluation: take polynomials $\Phi_{j\pm1}(x) = \Phi|_{I_{j\pm1}}$, and then sample in I_j to get $L[\Phi_j; \Phi_{j\pm1}, \eta]$ as defined in (48).
3. Evolution: obtain Φ^{n+1} from Φ^n by some Runge-Kutta type procedure to solve the ODE system (47).

In the AEDG schemes, ϵ is chosen such that the stability condition,

$$\Delta t \le \epsilon \le Q \frac{\Delta x}{\max |f'(u)|},$$

is satisfied. The choice of Q depends on the order of the scheme.

By a similar procedure one can construct AEDG schemes for multi-dimensional hyperbolic conservation laws:

$$\partial_t \phi + \nabla_x \cdot f(\phi) = 0, \quad x \in \mathbb{R}^d.$$

Again, let $\{x_\alpha\}$ be distributed grids in $\mathbb{R}^d$, and I_α be a hypercube centered at x_α with vertices at $x_{\alpha\pm1}$. Centered at each grid $\{x_\alpha\}$, the numerical approximation is a polynomial $\Phi|_{I_\alpha} = \Phi_\alpha(x) \in P_r$, where P_r denotes a linear space of all polynomials of degree at most r in all x_i:

$$P_r := \{p \mid p(x)|_{I_\alpha} = \sum_{0\le\beta_i\le r} a_\beta (x - x_\alpha)^\beta, \quad 1 \le i \le d, \quad a_\beta \in \mathbb{R}\}.$$

Integration of the AE system (32) over I_α against the test function $\eta \in P_r$, we obtain the semi-discrete AEDG scheme

$$\int_{I_\alpha} (\partial_t \Phi_\alpha + \nabla_x \cdot f(\Phi_\alpha^{SN}))\eta dx + \frac{1}{\epsilon}\int_{I_\alpha} \Phi_\alpha \eta dx = \frac{1}{\epsilon}\int_{I_\alpha} \Phi_\alpha^{SN}\eta dx - B, \tag{52}$$

$$B = \sum_{j=1}^{d} \int_{I_\alpha} [f(\Phi_\alpha^{SN})]\eta(x)\delta(x^j - x^j_{\alpha_j})dx, \tag{53}$$

where Φ_α^{SN} are sampled from neighboring polynomials. The choice of Φ_α^{SN} is not unique, and it is convenient to take the polynomials from the closest neighbors,

$$\Phi_\alpha^{SN} \in \text{span}\{\Phi_{\alpha\pm e_j}\}_{j=1}^d.$$

The way of sampling from neighboring polynomials for Hamilton-Jacobi equations can be applied well to the system of hyperbolic conservation laws.

6. Sample numerical experiments

The implementation of the AE algorithm began in [40], and further in [41, 42, 43]. Here sample numerical results are taken from [41, 42, 43], respectively.

In [41] we use some model problems of hyperbolic conservation laws to numerically test the first, second, and third order AE schemes as illustrated in section 2. Accuracy tests are based on scalar conservation laws such as the Burgers' equation, the nonlinear Buckley-Leverett problem, and multi-dimensional linear transport problems. For shock-capturing tests using the Euler equations of polytropic gas we compared the results with different initial data, including the Lax initial data, the Sod initial data, the Osher-Shu initial data, and the Woodward–Colella initial data. In all cases the resolution of the high order finite volume AE schemes is in good agreement with the established results in literature. One example is the explosion problem for the 2D Euler equation:

$$\phi_t + f(\phi)_x + g(\phi)_y = 0, \quad \phi = (\rho, \rho u, \rho v, E)^T, \quad p = (\gamma - 1)\left[E - \frac{\rho}{2}(u^2 + v^2)\right],$$
$$f(\phi) = (\rho u, \rho u^2 + p, \rho uv, u(E + p))^T, \quad g(\phi) = (\rho v, \rho uv, \rho v^2 + p, v(E + p))^T,$$

where $\gamma = 1.4$. This example chosen from [61] consists of a high density and high pressure region inside a bubble of radius 0.4 centered at the origin

Table 1: L^1, L^2, and L^∞ comparison for the non-convex Hamiltonian at time $t = \frac{0.5}{\pi^2}$ using 3rd order dimension-by-dimension AE scheme

N	Scheme	L^1 error	L^1 order	L^2 error	L^2 order	L^∞error	L^∞ order
20	AE	0.2885167659		0.0822233536		0.0445854569	
40	AE	0.0608972496	2.2442061801	0.0208873181	1.9769209512	0.0140420171	1.6668230099
80	AE	0.0122271144	2.3162931238	0.0044368628	2.2350153966	0.0034367453	2.0306353513
160	AE	0.0017583509	2.7977889587	0.0006572209	2.7550895638	0.0005444127	2.6582702568
320	AE	0.0002266868	2.9554505249	0.0000826895	2.9906021610	0.0000873968	2.6390477645
640	AE	0.0000273512	3.0510218754	0.0000097165	3.0891842742	0.0000111797	2.9666891406

and a low density and pressure region outside the bubble which causes the explosion. The initial data is

$$(p, \rho, u, v)(0) = \begin{cases} (1, 1, 0, 0) & x^2 + y^2 < 0.16, \\ (0.1, 0.125, 0, 0) & x^2 + y^2 \geq 0.16. \end{cases}$$

The solution is computed at time $T = 0.25$. In this experiment, constant extension boundary condition on all the four walls is used. CFL number used is 0.4 and time step is taken as $\Delta t = 0.95\epsilon$. In this test, the solution exhibits a circular shock and circular contact discontinuity moving away from the center of the circle and circular rarefaction wave moving in the opposite direction, a complex wave pattern emerging as time evolves. We compute this 2D bubble explosion solution by a second order AE scheme.

Presented in [42] are extensive numerical tests on both accuracy and capacity of high order finite difference AE schemes for solving Hamilton-Jacobi equations. For accuracy test, we take the example with a non-convex Hamiltonian:

$$\partial_t \phi - \cos(\partial_x \phi + \partial_y \phi + 1) = 0,$$

subject to initial data

$$\phi(x, y, 0) = -\cos\left(\frac{\pi(x + y)}{2}\right),$$

on the computation domain $[-2, 2]^2$ with periodic boundary conditions. At time $t = \frac{0.5}{\pi^2}$, the solution is still smooth and we test the order of accuracy for third order schemes using the dimension-by-dimension approach. The results in Table 1 show the desired order of accuracy in all norms.

For capacity of the scheme to capture the singularity, we test the Eikonal equation

$$\partial_t \phi + \sqrt{\partial_x \phi^2 + \partial_y \phi^2 + 1} = 0,$$

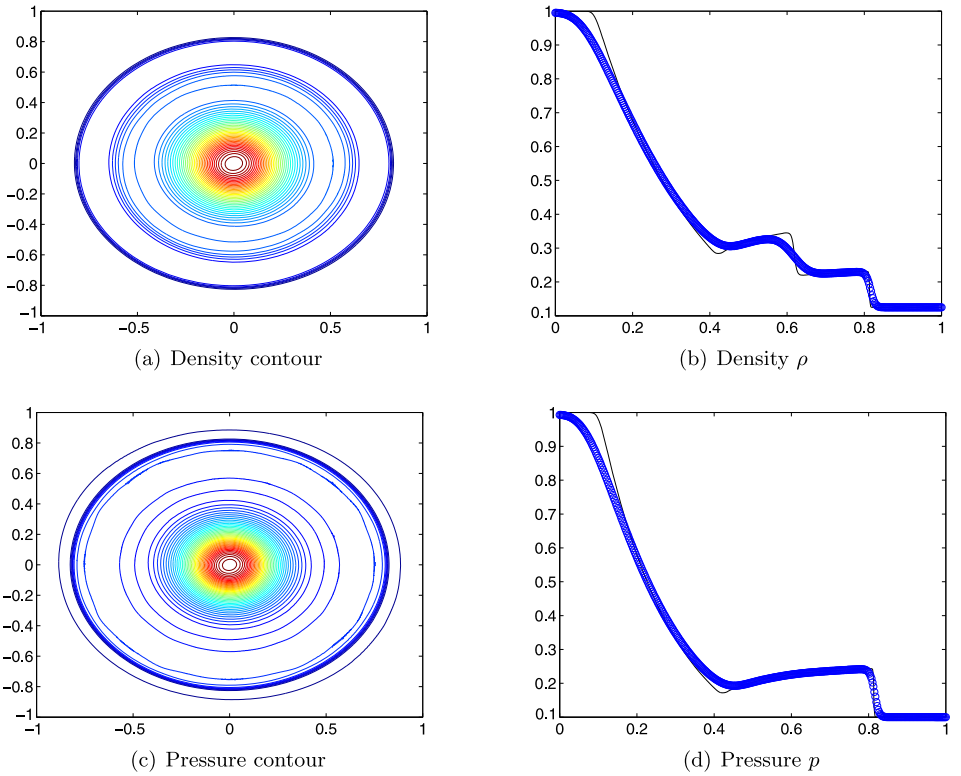

(a) Density contour (b) Density ρ

(c) Pressure contour (d) Pressure p

Figure 1: Isolines of density and pressure to the explosion problem (left). Comparison between the two dimensional solutions and the one dimensional radial solutions (right). **2nd order AE scheme** on $[-1,1]\times[-1,1]$, $T = 0.25$, $\Delta t = 0.95\epsilon$, $\Delta x = \Delta y = 1/400$.

with smooth initial data

$$\phi(x,y,0) = \frac{1}{4}\left(\cos(2\pi x) - 1\right)\left(\cos(2\pi y) - 1\right) - 1,$$

and computational domain $[0,1]^2$ and periodic boundary conditions. The results at time $t = 0.6$ are shown in Figure 2. The AE scheme provides high resolution in the formation of the singularity.

In [43], we tested both optimal accuracy and capacity of the AEDG algorithm for solving several time-dependent Hamilton-Jacobi equations. We here take one example relating to controlling optimal cost determination from [37, 22] with a nonsmooth Hamiltonian:

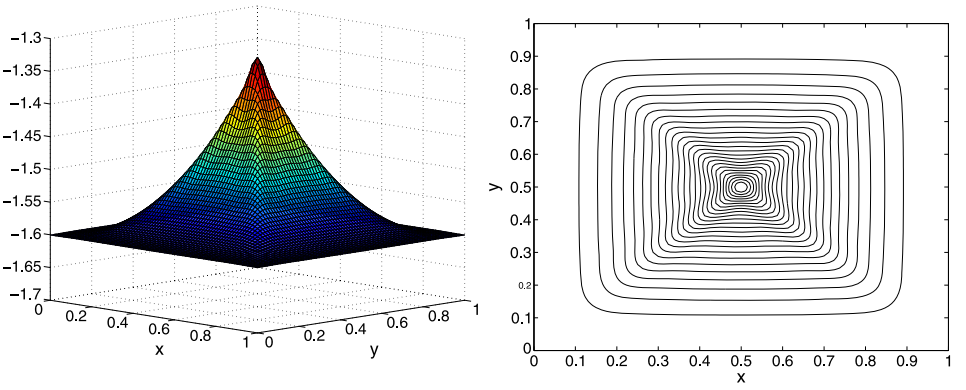

(a) AE scheme, $\Delta x = \Delta y = \frac{1}{80}$.

(b) AE scheme, $\Delta x = \Delta y = \frac{1}{80}$.

Figure 2: Surface and contour plots at time $t = 0.6$ for the 2D Eikonal equation.

$$\partial_t \Phi + \sin(y)\partial_x \Phi + (\sin(x) + \text{sign}(\partial_y \Phi))\partial_y \Phi - \frac{1}{2}\sin^2(y) + \cos(x) - 1 = 0,$$

with initial data $\Phi(x, y, 0) = 0$, on the computation domain $[-\pi, \pi]^2$ with periodic boundary conditions. The results for the numerical solution and optical control $\text{sign}(\partial_t \phi)$ are shown in Figure 3 using P^2 polynomials and are in agreement with those found in [37, 22].

7. Concluding remarks and future work

In this paper, we present a brief survey of the current state-of-the-art of AE methods for first order partial differential equations. We demonstrate the main ideas of the algorithm through two canonical model equations: hyperbolic conservation laws and Hamilton-Jacobi equations. We include some discussions of the properties and extensions of the schemes. Central solvers have recently gained growing attention in the field of conservation laws and Hamilton-Jacobi equations because of the guaranteed accuracy and reliable simulation results they provide. For both conservative and non-conservative PDEs we are able to apply the same discontinuous Galerkin framework upon the AE formulation. From the stand point of algorithm design and development, it would be interesting to explore ways to utilize fully the freedom of the AEDG framework such as hp-adaptivity. For practical purposes, we will develop AE models and solvers to simulate multi-phase fluids and problems involving multi-scales in the future. Extensions to both stationary Hamilton-

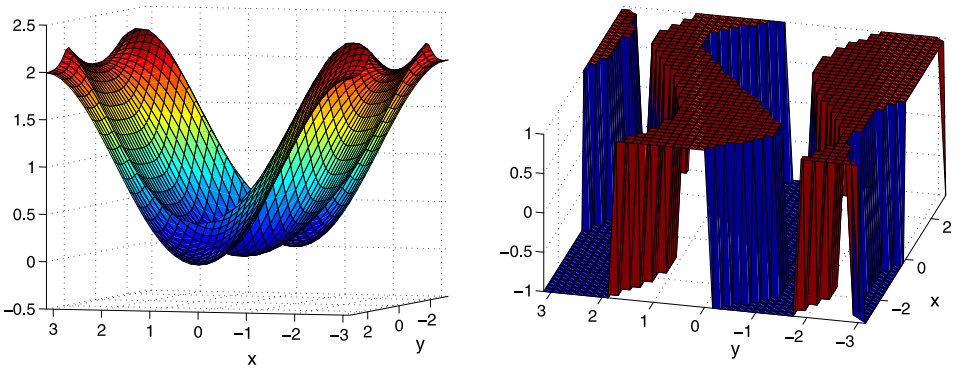

(a) Numerical Solution (b) Optimal Control

Figure 3: Numerical solution and optimal control plots at time $t = 1$ with $N_x = N_y = 81$ using P^2 polynomials.

Jacobi equations and the convection-diffusion equations using section 5.2 are currently underway.

In recent years, numerical solutions of fully nonlinear second order PDEs have attracted a great deal of attention from the numerical PDE and scientific communities, we refer to [15] for a recent review on this subject and references therein. Extension of our AE methods to second order fully nonlinear PDEs will also be an important component of our future research.

Acknowledgments

This research was partially supported by the National Science Foundation under grant DMS-1312636 and the KI-Net research network.

References

[1] F. Bianco, G. Puppo, and G. Russo. High-order central schemes for hyperbolic systems of conservation laws. *SIAM J. Sci. Comput.* 21(1):294–322 (electronic), 1999. MR1722134

[2] S. Bryson, A. Kurganov, D. Levy, and G. Petrova. Semi-discrete central-upwind schemes with reduced dissipation for Hamilton-Jacobi equations. *IMA J. Numer. Anal.* 25(1):113–138, 2005. MR2110237

[3] S. Bryson and D. Levy. High-order central WENO schemes for multidimensional Hamilton-Jacobi equations. *SIAM J. Numer. Anal.* 41(4):1339–1369 (electronic), 2003. MR2034884

[4] S. Bryson and D. Levy. High-order semi-discrete central-upwind schemes for multi-dimensional Hamilton-Jacobi equations. *J. Comput. Phys.* 189(1):63–87, 2003. MR1988140

[5] M. G. Crandall, L. C. Evans, and P. L. Lions. Some properties of viscosity solutions of Hamilton-Jacobi equations. *Trans. Amer. Math. Soc.* 282:487–502, 1984. MR0732102

[6] Y. Cheng and C.-W. Shu. A discontinuous Galerkin finite element method for directly solving the Hamilton-Jacobi equations. *J. Comput. Phys.* 223(1):398–415, 2007. MR2314396

[7] B. Cockburn and C.-W. Shu. Runge-Kutta discontinuous Galerkin methods for convection-dominated problems. *J. Sci. Comput.* 16(3): 173–261, 2001. MR1873283

[8] P. Colella and P. R. Woodward. The piecewise parabolic method (PPM) for gas-dynamical simulations. *J. Comput. Phys.* 54(1):174–201, 1984.

[9] M. G. Crandall and P.-L. Lions. Viscosity solutions of Hamilton-Jacobi equations. *Trans. Amer. Math. Soc.* 277(1):1–42, 1983. MR0690039

[10] B. Cockburn, S. Hou, and C.-W. Shu. The Runge-Kutta local projection discontinuous Galerkin finite element method for conservation laws. IV. The multidimensional case. *Math. Comput.* 54(190):545–581, 1990. MR1010597

[11] B. Cockburn, S. Y. Lin, and C.-W. Shu. TVB Runge-Kutta local projection discontinuous Galerkin finite element method for conservation laws. III. One-dimensional systems. *J. Comput. Phys.* 84(1):90–113, 1989. MR1015355

[12] B. Cockburn and C.-W. Shu. TVB Runge-Kutta local projection discontinuous Galerkin finite element method for conservation laws. II. General framework. *Math. Comput.* 52(186):411–435, 1989. MR0983311

[13] B. Cockburn and C.-W. Shu. The Runge-Kutta local projection P^1 discontinuous Galerkin finite element method for scalar conservation laws. RAIRO model. *Math. Anal. Numer* 25(3):337–361, 1991. MR1103092

[14] B. Cockburn and C.-W. Shu. The Runge-Kutta discontinuous Galerkin method for conservation laws. V. Multidimensional systems. *J. Comput. Phys.* 141(2):199–224, 1998. MR1619652

[15] X.-B. Feng, R. Glowinski, and M. Neilan. Recent developments in numerical methods for fully nonlinear second order partial differential equations. *SIAM Review* 55(2):205–267, 2013. MR3049920

[16] K. O. Friedrichs. Symmetric hyperbolic linear differential equations. *Comm. Pure Appl. Math.* 7:345–392, 1954. MR0062932

[17] S. K. Godunov. A difference method for numerical calculation of discontinuous solutions of the equations of hydrodynamics. *Mat. Sb. (N.S.)* 47(89):271–306, 1959. MR0119433

[18] S. Gottlieb, C.-W. Shu, and E. Tadmor. Strong stability-preserving high-order time discretization methods. *SIAM Rev.* 43(1):89–112 (electronic), 2001. MR1854647

[19] A. Harten. High resolution schemes for hyperbolic conservation laws. *J. Comput. Phys.* 49(3):357–393, 1983. MR0701178

[20] A. Harten, B. Engquist, S. Osher, and S. R. Chakravarthy. Uniformly high-order accurate essentially nonoscillatory schemes. III. *J. Comput. Phys.* 71(2):231–303, 1987. MR0897244

[21] A. Harten, P. D. Lax, and B. van Leer. On upstream differencing and Godunov-type schemes for hyperbolic conservation laws. *SIAM Rev.* 25(1):35–61, 1983. MR0693713

[22] C. Hu and C.-W. Shu. A discontinuous Galerkin finite element method for Hamilton-Jacobi equations. *SIAM J. Sci. Comput.* 21(2):666–690 (electronic), 1999. MR1718679

[23] G.-S. Jiang, D. Levy, C.-T. Lin, S. Osher, and E. Tadmor. High-resolution nonoscillatory central schemes with nonstaggered grids for hyperbolic conservation laws. *SIAM J. Numer. Anal.* 35(6):2147–2168 (electronic), 1998. MR1655841

[24] G.-S. Jiang and D. Peng. Weighted ENO schemes for Hamilton-Jacobi equations. *SIAM J. Sci. Comput.* 21(6):2126–2143 (electronic), 2000. MR1762034

[25] G.-S. Jiang and E. Tadmor. Nonoscillatory central schemes for multidimensional hyperbolic conservation laws. *SIAM J. Sci. Comput.* 19(6):1892–1917 (electronic), 1998. MR1638064

[26] S. Jin and Z. P. Xin. The relaxation schemes for systems of conservation laws in arbitrary space dimensions. *Comm. Pure Appl. Math.* 48(3):235–276, 1995. MR1322811

[27] M. A. Katsoulakis and A. E. Tzavaras. Contractive relaxation systems and interacting particles for scalar conservation laws. *C. R. Acad. Sci. Paris Sér. I Math.* 323(8):865–870, 1996. MR1414549

[28] A. Kurganov and C.-T. Lin. On the reduction of numerical dissipation in central-upwind schemes. *Commun. Comput. Phys.* 2(1):141–163, 2007. MR2305919

[29] A. Kurganov, S. Noelle, and G. Petrova. Semidiscrete central-upwind schemes for hyperbolic conservation laws and Hamilton-Jacobi equations. *SIAM J. Sci. Comput.* 23(3):707–740 (electronic), 2001. MR1860961

[30] A. Kurganov and G. Petrova. A third-order semi-discrete genuinely multidimensional central scheme for hyperbolic conservation laws and related problems. *Numer. Math.* 88(4):683–729, 2001. MR1836876

[31] A. Kurganov and E. Tadmor. New high-resolution central schemes for nonlinear conservation laws and convection-diffusion equations. *J. Comput. Phys.* 160(1):241–282, 2000. MR1756766

[32] A. Kurganov and E. Tadmor. New high-resolution semi-discrete central schemes for Hamilton-Jacobi equations. *J. Comput. Phys.* 160(2):720–742, 2000. MR1763829

[33] P. D. Lax. Weak solutions of nonlinear hyperbolic equations and their numerical computation. *Comm. Pure Appl. Math.* 7:159–193, 1954. MR0066040

[34] R. J. LeVeque. *Numerical methods for conservation laws.* Lectures in Mathematics ETH Zürich. Birkhäuser Verlag, Basel, second edition, 1992. MR1153252

[35] D. Levy, S. Nayak, C.-W. Shu, and Y.-T. Zhang. Central WENO schemes for Hamilton-Jacobi equations on triangular meshes. *SIAM J. Sci. Comput.* 28(6):2229–2247 (electronic), 2006. MR2272259

[36] D. Levy, G. Puppo, and G. Russo. Central WENO schemes for hyperbolic systems of conservation laws. *M2AN Math. Model. Numer. Anal.* 33(3):547–571, 1999. MR1713238

[37] F. Y. Li and S. Yakovlev. A central discontinuous Galerkin method for Hamilton-Jacobi equations. *J. Sci. Comput.* 45(1-3), 404–428, 2010. MR2679806

[38] C.-T. Lin and E. Tadmor. High-resolution nonoscillatory central schemes for Hamilton-Jacobi equations. *SIAM J. Sci. Comput.* 21(6): 2163–2186 (electronic), 2000. MR1762036

[39] C.-T. Lin and E. Tadmor. L^1-Stability and error estimates for approximate Hamilton-Jacobi solutions. *Numer. Math.* 87:701–735, 2001. MR1815732

[40] H. Liu. An alternating evolution approximation to systems of hyperbolic conservation laws. *J. Hyperbolic Differ. Equ.* 5(2):421–447, 2008. MR2420005

[41] H. Saran and H. Liu. Formulation and analysis of alternating evolution schemes for conservation laws. *SIAM J. Sci. Comput.* 33:3210–3240, 2011. MR2862011

[42] H. Liu, M. Pollack, and H. Saran. Alternating evolution schemes for Hamilton–Jacobi equations. *SIAM J. Sci. Comput.* 35(1):122–149, 2013. MR3033040

[43] H. Liu and M. Pollack. Alternating evolution DG methods for Hamilton-Jacobi equations. *J. Comput. Phys.* 258:32–46, 2014. MR3145268

[44] X.-D. Liu, S. Osher, and T. Chan. Weighted essentially non-oscillatory schemes. *J. Comput. Phys.* 115(1):200–212, 1994. MR1300340

[45] X.-D. Liu and E. Tadmor. Third order nonoscillatory central scheme for hyperbolic conservation laws. *Numer. Math.* 79(3):397–425, 1998. MR1626324

[46] Y. Liu. Central schemes on overlapping cells. *J. Comput. Phys.* 209(1): 82–104, 2005. MR2145783

[47] Y.-J. Liu, C.-W. Shu, E. Tadmor, and M.-P. Zhang. Central discontinuous Galerkin methods on overlapping cells with a non-oscillatory hierarchical reconstruction. *SIAM J. Numer. Anal.* 45:2442–2467, 2007. MR2361897

[48] Y.-J. Liu, C.-W. Shu, E. Tadmor, and M.-P. Zhang. Non-oscillatory hierarchical reconstruction for central and finite volume schemes. *Communications in Computational Physics* 2:933–963, 2007. MR2355632

[49] Y. Liu, C.-W. Shu, E. Tadmor, and M.-P. Zhang. L2 stability analysis of the central discontinuous Galerkin method and a comparison between the central and regular discontinuous Galerkin methods *ESAIM: Mathematical Modelling and Numerical Analysis* 42:593–607, 2008. MR2437775

[50] Y.-J. Liu, C.-W. Shu, E. Tadmor, and M.-P. Zhang. Central local discontinuous Galerkin methods on overlapping cells for diffusion

equations. *ESAIM: Mathematical Modelling and Numerical Analysis* 45:1009–1032, 2011. MR2833171

[51] R. Natalini. A discrete kinetic approximation of entropy solutions to multidimensional scalar conservation laws. *J. Differential Equations* 148(2):292–317, 1998. MR1643175

[52] H. Nessyahu and E. Tadmor. Nonoscillatory central differencing for hyperbolic conservation laws. *J. Comput. Phys.* 87(2):408–463, 1990. MR1047564

[53] J. Qiu and C. W. Shu. Hermite WENO schemes for Hamilton-Jacobi equations. *J. Comput. Phys.* 204:82–99, 2005. MR2121905

[54] S. Osher and J. A. Sethian. Fronts propagating with curvature-dependent speed: algorithms based on Hamilton-Jacobi formulations. *J. Comput. Phys.* 79(1):12–49, 1988. MR0965860

[55] S. Osher and C.-W. Shu. High-order essentially nonoscillatory schemes for Hamilton-Jacobi equations. *SIAM J. Numer. Anal.* 28(4):907–922, 1991. MR1111446

[56] C.-W. Shu. High order ENO and WENO schemes for computational fluid dynamics. in: *High-order methods for computational physics*, Lect. Notes Comput. Sci. Eng., Vol. 9, Springer, Berlin, 1999, pp. 439–582. MR1712281

[57] C.-W. Shu and S. Osher. Efficient implementation of essentially nonoscillatory shock-capturing schemes. *J. Comput. Phys.* 77(2):439–471, 1988. MR0954915

[58] C.-W. Shu and S. Osher. Efficient implementation of essentially nonoscillatory shock-capturing schemes. II. *J. Comput. Phys.* 83(1):32–78, 1989. MR1010162

[59] P. E. Souganidis. Approximation schemes for viscosity solutions of Hamilton-Jacobi equations. *J. Differ. Equ.* 59:1ÔŅĹ43, 1985. MR0803085

[60] E. Tadmor. Approximate solutions of nonlinear conservation laws and related equations. in: *Recent advances in partial differential equations, Venice 1996*, Proc. Sympos. Appl. Math., Vol. 54, Amer. Math. Soc., Providence, RI, 1998, pp. 325–368. MR1492703

[61] E. F. Toro. *Riemann solvers and numerical methods for fluid dynamics.* Springer-Verlag, Berlin, second edition, 1999. A practical introduction. MR1717819

[62] B. van Leer. Upwind differencing for hyperbolic systems of conservation laws. in: *Numerical methods for engineering, 1 (Paris, 1980)*, Dunod, Paris, 1980, pp. 137–149. MR0660670

[63] B. van Leer. Towards the ultimate conservative difference scheme. V. A second-order sequel to Godunov's method [J. Comput. Phys. **32** (1979), no. 1, 101–136]. *J. Comput. Phys.* 135(2):227–248, 1997. With an introduction by Ch. Hirsch, Commemoration of the 30th anniversary of J. Comput. Phys. MR1486274

[64] J. Yan and S. Osher. A new discontinuous Galerkin method for Hamilton-Jacobi equations. *J. Comput. Phys.* 230(1):232–244, 2011. MR2734289

[65] Y.-T. Zhang and C.-W. Shu. High order WENO schemes for Hamilton-Jacobi equations on triangular meshes. *SIAM J. Sci. Comput.* 24:1005–1030, 2003. MR1950522

Hailiang Liu
Department of Mathematics
Iowa State University
Ames, Iowa 50010
USA
E-mail address: hliu@iastate.edu

Received September 24, 2013